Journal of Process Control 92 (2020) 108–118

Contents lists available at ScienceDirect

Journal of Process Control

journal homepage: www.elsevier.com/locate/jprocont

Adaptive horizon economic nonlinear model predictive control ☆

Dinesh Krishnamoorthy [a], Lorenz T. Biegler [b], Johannes Jäschke [a,*]

[a] Department of Chemical Engineering, Norwegian University of Science and Technology (NTNU), Trondheim, Norway
[b] Department of Chemical Engineering, Carnegie Mellon University, Pittsburgh, PA, 15213, USA

ARTICLE INFO

Article history:
Received 27 December 2019
Received in revised form 21 May 2020
Accepted 28 May 2020
Available online 12 June 2020

Keywords:
Economic model predictive control
Fast MPC
Sensitivity
Dynamic optimization
Process control

ABSTRACT

In this paper, we present a computationally efficient economic NMPC formulation, where we propose to adaptively update the length of the prediction horizon in order to reduce the problem size. This is based on approximating an infinite horizon economic NMPC problem with a finite horizon optimal control problem with terminal region of attraction to the optimal equilibrium point. Using the nonlinear programming (NLP) sensitivity calculations, the minimum length of the prediction horizon required to reach this terminal region is determined. We show that the proposed adaptive horizon economic NMPC (AH-ENMPC) has comparable performance to standard economic NMPC (ENMPC). We also show that the proposed adaptive horizon economic NMPC framework is nominally stable. Two benchmark examples demonstrate that the proposed adaptive horizon economic NMPC provides similar performance as the standard economic NMPC with significantly less computation time.

1. Introduction

Real time optimization (RTO) and model predictive control (MPC) have emerged as crucial technologies in achieving online process optimization. Traditionally, real time optimization (RTO) focuses on the steady-state optimal economic operation. Recently there is an increasing interest in not only ensuring that the process is operated optimally at steady-state, but that transients are optimized as well. This is done in the context of dynamic real time optimization (DRTO) [1], which provides the optimal setpoint trajectories to the control layer below, which are often implemented using model predictive control (MPC). Moreover, MPC has also evolved to nonlinear model predictive control (NMPC) to ensure reliable control of highly nonlinear systems. More recently, the DRTO and NMPC layers have been tightly integrated into a single layer approach, known as economic NMPC [2], where there is no time scale separation such as in the conventional two-layer approach.

DRTO, NMPC, and the closely related economic NMPC are all based on using a dynamic model of the process to solve numerical optimization problems online, in order to minimize a desired objective function. Realizing these tasks in real time requires fast optimization algorithms. As many industrial applications call for increasingly complex, detailed and large-scale process models [3], a major concern is the computational resources needed to solve the resulting large-scale optimization problem. While advances in numerical optimization strategies have enabled us to solve increasingly larger optimal control problems (OCPs), real-time implementation is still challenging, even with today's computing power [4,5]. The non-negligible amount of time required to solve the numerical optimization problem online leads to computational delays, which are known to degrade the control performance [6] and can also destabilize the system [7,8].

One of the main reasons for computational delay is the optimization problem size, which increases with the prediction horizon. Typically, the prediction horizon is chosen to be conservatively long in order to ensure feasibility and stability of the dynamic optimization problem [9]. However, when using an economic NMPC framework, as opposed to a two-layer framework with dynamic RTO and setpoint tracking control layer, it may be desirable to implement the economic MPC at higher sampling rates [10] and the sampling time is limited by the worst-case computation delay. Thus reducing the online computation delay is important for implementation of economic NMPC at higher sampling rates.

Shekhar [11] proposed a variable horizon MPC formulation, where the prediction horizon length itself is a decision variable. Since the horizon length is an integer variable, this leads to a mixed integer nonlinear programming problem (MINLP) for the economic NMPC. For large-scale systems, such an approach is impractical and more computationally intensive than solving an NLP with long prediction horizon.

☆ The authors gratefully acknowledge the financial support from SUBPRO , which is financed by the Research Council of Norway, major industry partners and NTNU.

* Corresponding author.
E-mail addresses: dinesh.krishnamoorthy@ntnu.no (D. Krishnamoorthy), lb01@andrew.cmu.edu (L.T. Biegler), johannes.jaschke@ntnu.no (J. Jäschke).

https://doi.org/10.1016/j.jprocont.2020.05.013

Recently, an adaptive horizon NMPC problem was proposed in [9], where the length of the prediction horizon is chosen in real-time based on the current state, and terminal conditions are enforced to approximate the infinite horizon problem. In this paper, we use the idea of dissipativity to extend the adaptive horizon NMPC problem formulation to the economic NMPC problem, by enforcing a region of attraction to the optimal equilibrium point as a terminal constraint. By doing so, we only need to compute the optimal trajectory to this terminal region online. The NLP sensitivity updates are used to choose the prediction horizon length in real-time.

The main contribution of this paper, is the extension of the adaptive horizon NMPC [9] to economic NMPC problems, such that the stability properties are retained. The rest of the paper is organized as follows. Section 2 introduces the problem formulation and the preliminaries. Section 3 introduces the computation of the terminal region of attraction to the optimal equilibrium point. The algorithm to update the horizon length online is detailed in Section 4. Stability analysis is performed in Section 5. Section 6 demonstrates the performance of the proposed adaptive horizon economic NMPC on a CSTR process and Section 7 demonstrates the performance of the proposed approach on a benchmark Williams–Otto reactor, before concluding the paper in Section 8.

2. Preliminaries

We consider a discrete time nonlinear model

$$\mathbf{x}_{k+1} = \mathbf{f}(\mathbf{x}_k, \mathbf{u}_k) \tag{1}$$

where, the states $\mathbf{x} \in \mathcal{X}$ and the control inputs $\mathbf{u} \in \mathcal{U}$ at time k are constrained to lie in the compact sets $\mathcal{X} \subset \mathbb{R}^{n_x}$ and $\mathcal{U} \subset \mathbb{R}^{n_u}$ respectively. The nominal plant model denoted by $\mathbf{f} : \mathcal{X} \times \mathcal{U} \to \mathcal{X}$ is assumed to be twice differentiable in $\mathbf{x}$ and $\mathbf{u}$.

The objective is to control the plant to achieve optimal economic operation and we consider an economic NMPC scheme based on receding horizon formulation to achieve this. At time step t, the optimal control problem (OCP) is formulated as,

$$V_N(\hat{\mathbf{x}}_t) := \min_{\mathbf{x}_k, \mathbf{u}_k} V_f(\mathbf{x}_N) + \sum_{k=0}^{N-1} \ell(\mathbf{x}_k, \mathbf{u}_k) \tag{2a}$$

s.t.

$$\mathbf{x}_{k+1} = \mathbf{f}(\mathbf{x}_k, \mathbf{u}_k) \tag{2b}$$

$$\mathbf{x}_0 = \hat{\mathbf{x}}_t \tag{2c}$$

$$\mathbf{x}_k \in \mathcal{X}, \quad \mathbf{u}_k \in \mathcal{U}, \quad \mathbf{x}_N \in \mathcal{X}_f \quad \forall k \in \{0, \dots, N-1\} \tag{2d}$$

where, the stage cost is denoted by $\ell(\cdot,\cdot) : \mathcal{X} \times \mathcal{U} \to \mathbb{R}$ that typically contains economic terms along with a terminal penalty $V_f : \mathcal{X}_f \to \mathbb{R}$ that accounts for the truncation of the prediction horizon after N steps. The OCP is solved with $\hat{\mathbf{x}}_t$ as the initial condition, which is the actual plant state measurement or estimate at time step t, and the first control input is implemented on the plant, i.e. $\boldsymbol{\mu}_t(\hat{\mathbf{x}}_t) := \mathbf{u}_0$.

Notational remarks. We use the notation $\hat{\mathbf{x}}_t$ to denote the measured state and $\boldsymbol{\mu}_t$ to denote the input implemented on the system at time step t. $\hat{\mathbf{x}}_{t+1|t}$ denotes the states at $t+1$ predicted at time step t using the plant model (1). We denote the dependence of the optimal control problem (2) on the initial condition $\hat{\mathbf{x}}_t$ and the horizon length N by writing $OCP_N(\hat{\mathbf{x}}_t)$. The time step in the optimal control problem (2) is given by $k \in \{0, \dots, N-1\}$. For a given control sequence $\mathbf{u} = (\mathbf{u}_0, \mathbf{u}_1, \dots, \mathbf{u}_{N-1}) \in \mathcal{U}$, $\mathbf{x}_k(\mathbf{u}, \hat{\mathbf{x}}_t)$ denotes the solution of (1) with the initial condition $\mathbf{x}_0 = \hat{\mathbf{x}}_t$ at any time step $k \in \{0, \dots, N\}$. The optimal control sequence dependent on the initial condition $\hat{\mathbf{x}}_t$ is denoted as $\mathbf{u}(\cdot, \hat{\mathbf{x}}_t)^*$. We use $|\cdot|$ to denote an Euclidean vector norm.

Suppose (2) is re-written in the standard NLP form,

$$\min_{\mathbf{w}} J(\mathbf{w}) \quad \text{s.t} \quad \mathbf{g}(\mathbf{w}) \le 0, \ \mathbf{c}(\mathbf{w}) = 0 \tag{3}$$

with $\mathbf{w} := [\mathbf{u}_0, \mathbf{x}_1, \dots, \mathbf{u}_{N-1}, \mathbf{x}_N]$, (2a) denoted by $J(\mathbf{w})$, (2b) and (2c) denoted by $\mathbf{c}(\mathbf{w})$ and (2d) denoted by $\mathbf{g}(\mathbf{w})$, we can define constraint qualifications and second order sufficient conditions as follows.

Definition 1 (*MFCQ*)**.** The Mangasarian–Fromovitz constraint qualification (MFCQ) is said to hold at an optimal point $\mathbf{w}^*$ if and only if, $\nabla_{\mathbf{w}}\mathbf{c}(\mathbf{w}^*)$ has full column rank (linearly independent) and, there exists a direction $\mathbf{d} \neq 0$, such that $\nabla_{\mathbf{w}}\mathbf{c}(\mathbf{w}^*)^T\mathbf{d} = 0$ and $\nabla_{\mathbf{w}}\mathbf{g}_i(\mathbf{w}^*)^T\mathbf{d} < 0$ for all i such that $\mathbf{g}_i(\mathbf{w}^*) = 0$ (active inequality constraints).

Definition 2 (*GSSOSC*)**.** Suppose $\nabla^2_{\mathbf{ww}}\mathcal{L}$ is the Hessian of the Lagrangian of (3) and, λ, μ are the multipliers of $\mathbf{c}$ and $\mathbf{g}$ respectively. The generalized strong second order sufficient condition (GSSOSC) is said to hold at a first order KKT point $\mathbf{w}^*$ if for all directions $\mathbf{d}$ for all i such that $\nabla_{\mathbf{w}}\mathbf{g}_i(\mathbf{w}^*)^T\mathbf{d} = 0$ and $\mu_i^* > 0$ (i.e, strongly active inequality constraints), $\mathbf{d}^T\nabla^2_{\mathbf{ww}}\mathcal{L}(\mathbf{w}^*, \lambda^*, \mu^*)\mathbf{d} > 0$ is satisfied for all multipliers λ and μ.

We now make the following assumptions.

Assumption 1. The set $\mathcal{X}$ is assumed to be control positive invariant for $\mathbf{f}(\cdot,\cdot)$, that is for each $\mathbf{x} \in \mathcal{X}$, there exists a control $\mathbf{u} \in \mathcal{U}$ such that $\mathbf{f}(\mathbf{x}, \mathbf{u}) \in \mathcal{X}$.

Assumption 2. $\mathcal{X} \times \mathcal{U}$ is compact and the functions $\mathbf{f} : \mathcal{X} \times \mathcal{U} \to \mathcal{X}$ and $\ell : \mathcal{X} \times \mathcal{U} \to \mathbb{R}$ are twice differentiable.

Assumption 3. MFCQ and GSSOSC holds for the optimal control problem in (2).

Satisfying Assumption 1 is dependent on the process system and choice of controller. In our case, if Assumptions 2 and 3 hold for NMPC controller based on (2), then Assumption 1 holds. Assumption 3 implies that the primal solution $\mathbf{w}^*$ of (2) is locally unique.

Definition 3 (*$\mathcal{K}$-Functions*)**.** A function $\alpha : \mathbb{R}_+ \to \mathbb{R}_+$ is of class $\mathcal{K}$, if it is continuous and strictly increasing with $\alpha(0) = 0$. Further it is of class $\mathcal{K}_\infty$ if α is unbounded.

Definition 4 (*Optimal Equilibrium Pair*)**.** A pair $(\mathbf{x}, \mathbf{u}) \in \mathcal{X} \times \mathcal{U}$ is called an equilibrium or steady-state pair if $\mathbf{x} = \mathbf{f}(\mathbf{x}, \mathbf{u})$ holds. Furthermore, an equilibrium pair $(\mathbf{x}_f, \mathbf{u}_f) \in \mathcal{X} \times \mathcal{U}$ is called an optimal equilibrium pair if it yields the lowest value of the cost among all the equilibrium points

$$\ell(\mathbf{x}_f, \mathbf{u}_f) \le \ell(\mathbf{x}, \mathbf{u}) \ \ \forall (\mathbf{x}, \mathbf{u}) \in \mathcal{X} \times \mathcal{U} \text{ with } \mathbf{x} = \mathbf{f}(\mathbf{x}, \mathbf{u}) \tag{4}$$

Assumption 2 guarantees the existence of such an optimal equilibrium point, as shown in [12, Lemma 8.4].

Definition 5 (*Dissipativity*)**.** System $\mathbf{x}_{k+1} = \mathbf{f}(\mathbf{x}_k, \mathbf{u}_k)$ is said to be dissipative w.r.t a steady-state pair $(\mathbf{x}_f, \mathbf{u}_f) \in \mathcal{X} \times \mathcal{U}$, if $\exists \boldsymbol{\lambda} : \mathcal{X} \to \mathbb{R}^+$ such that for all $\mathbf{x} \in \mathcal{X}$ and $\mathbf{u} \in \mathcal{U}$,

$$\boldsymbol{\lambda}(\mathbf{f}(\mathbf{x}, \mathbf{u})) - \boldsymbol{\lambda}(\mathbf{x}) \le s(\mathbf{x}, \mathbf{u}) \tag{5}$$

Here, $\boldsymbol{\lambda}$ is the storage function and $s(\mathbf{x}, \mathbf{u}) := \ell(\mathbf{x}, \mathbf{u}) - \ell(\mathbf{x}_f, \mathbf{u}_f)$ is the supply rate, and without loss of generality we assume $\ell(\mathbf{x}, \mathbf{u}) \ge 0$ for all $(\mathbf{x}, \mathbf{u}) \in \mathcal{X} \times \mathcal{U}$.

Definition 6 (*Strict Dissipativity*). System $\mathbf{x}_{k+1} = \mathbf{f}(\mathbf{x}_k, \mathbf{u}_k)$ is said to be strictly dissipative w.r.t $(\mathbf{x}_f, \mathbf{u}_f) \in \mathcal{X} \times \mathcal{U}$, if in addition to Definition 5, $\exists\ \alpha_l \in \mathcal{K}_\infty$ such that

$$\boldsymbol{\lambda}(\mathbf{f}(\mathbf{x}, \mathbf{u})) - \boldsymbol{\lambda}(\mathbf{x}) \leq -\alpha_l(|\mathbf{x} - \mathbf{x}_f|) + s(\mathbf{x}, \mathbf{u}) \tag{6}$$

Assumption 4. (a) There exists at least one steady-state pair $(\mathbf{x}_f, \mathbf{u}_f) \in \mathcal{X} \times \mathcal{U}$ such that $\mathbf{x}_f = \mathbf{f}(\mathbf{x}_f, \mathbf{u}_f)$ holds. (b) There exists a bounded non-negative storage function $\boldsymbol{\lambda} : \mathcal{X} \to \mathbb{R}^+$ and $\alpha_l \in \mathcal{K}_\infty$, such that the OCP (2) is strictly dissipative w.r.t the steady-state pair $(\mathbf{x}_f, \mathbf{u}_f)$ in the sense of Definition 6, where $s(\mathbf{x}, \mathbf{u}) := \ell(\mathbf{x}, \mathbf{u}) - \ell(\mathbf{x}_f, \mathbf{u}_f)$.

Lemma 1. *Given Assumptions 3 and 4, $(\mathbf{x}_f, \mathbf{u}_f)$ is a unique global minimizer of the steady-state optimization problem*

$$(\mathbf{x}_f, \mathbf{u}_f) = arg \min_{\mathbf{x},\mathbf{u}} \ell(\mathbf{x}, \mathbf{u}) \tag{7a}$$

s.t.

$$\mathbf{x} = \mathbf{f}(\mathbf{x}, \mathbf{u}) \tag{7b}$$

$$\mathbf{x} \in \mathcal{X},\ \ \mathbf{u} \in \mathcal{U} \tag{7c}$$

Proof. This can be proved by contradiction. If $(\mathbf{x}_f, \mathbf{u}_f)$ is not the global minimizer, then there exists another equilibrium pair $(\mathbf{x}_e, \mathbf{u}_e)$ such that $\ell(\mathbf{x}_e, \mathbf{u}_e) < \ell(\mathbf{x}_f, \mathbf{u}_f)$. Evaluating the dissipation inequality in (5) at $(\mathbf{x}_e, \mathbf{u}_e)$ gives, $\ell(\mathbf{x}_f, \mathbf{u}_f) \leq \ell(\mathbf{x}_e, \mathbf{u}_e)$. This leads to a contradiction.

Evaluating the strict dissipation inequality (6) at $(\mathbf{x}_e, \mathbf{u}_e)$ gives, $0 < \alpha_l(|\mathbf{x}_e - \mathbf{x}_f|) \leq \ell(\mathbf{x}_e, \mathbf{u}_e) - \ell(\mathbf{x}_f, \mathbf{u}_f)$. Hence $\ell(\mathbf{x}_f, \mathbf{u}_f)$ is the unique global minimizer. □

Strict dissipativity implies that the system is optimally operated at steady-state, which is formalized below.

Proposition 1. *Given Assumption 4 and Lemma 1, the inequality*

$$\limsup_{T\to\infty} \frac{1}{T} \sum_{k=0}^{T-1} \ell(\mathbf{x}_k(\mathbf{u}(\hat{\mathbf{x}}_t), \hat{\mathbf{x}}_t), \mathbf{u}_k(\hat{\mathbf{x}}_t)) \geq \ell(\mathbf{x}_f, \mathbf{u}_f) \tag{8}$$

holds for all $\mathbf{x}_k \in \mathcal{X}$ and all admissible control sequences $\mathbf{u}_k \in \mathcal{U}$.

Proof. See [12, Proposition 8.9] or [13, Proposition 6.4]. □

The inequality (8) expresses that the system is optimally operated at steady-state (sub-optimally operated off steady-state) [12, 13]. As shown in [14] dissipativity is a sufficient condition for optimal operation at steady-state, and the convergence analysis using the dissipativity condition in [13,15] showed that the closed-loop system does converge to the optimal steady-state.

Furthermore, if the optimal equilibrium point is exponentially reachable, then it was shown in [16,17], that strict dissipativity and exponential reachability implies that the optimal solution of the OCP spends most of the time in an ε-neighborhood to the optimal equilibrium pair $(\mathbf{x}_f, \mathbf{u}_f)$, (also known as turnpike property). For any initial condition $\hat{\mathbf{x}}_t \in \mathcal{X}$, once the optimal equilibrium $(\mathbf{x}_f, \mathbf{u}_f)$ is reached, the tail subproblem starting from $(\mathbf{x}_f, \mathbf{u}_f)$ is identical, which follows directly from Bellman's principle of optimality.

To summarize in simple words, we have thus far established that there exists an optimal equilibrium point $(\mathbf{x}_f, \mathbf{u}_f)$, and that the system is optimally operated at steady-state $(\mathbf{x}_f, \mathbf{u}_f)$. Furthermore, for any initial condition $\hat{\mathbf{x}}_t$ starting from a control invariant compact set $\mathcal{X}$, the optimal solution of the OCP (2) exponentially converges to the optimal equilibrium point $(\mathbf{x}_f, \mathbf{u}_f)$. With this we now propose to adaptively update the length of the prediction horizon of the OCP (2), in order to reduce the problem size and consequently reduce the online computation time.

The key idea here is to find a terminal region of attraction $\mathcal{X}_f$ which contains the optimal equilibrium point $(\mathbf{x}_f, \mathbf{u}_f)$. If one can then ensure that a stabilizing control law exists within this terminal region, such that the system will asymptotically converge to the optimal equilibrium point from any $\mathbf{x} \in \mathcal{X}_f$, then OCP (2) only needs to be solved with the minimum number of samples required to reach the terminal region $\mathcal{X}_f$, along with a terminal cost that approximates the infinite horizon economic NMPC problem. In other words, we modify the original OCP (2) with a reduced prediction horizon length and add a Lyapunov function as the terminal cost. This is described in more detail in the next section.

3. Quasi-infinite economic NMPC with terminal constraints

In this section, we describe the problem of finding a region of attraction $\mathcal{X}_f$, such that for any $\mathbf{x} \in \mathcal{X}_f$, there exists a stabilizing control law $\mathbf{u} = \kappa_f(\mathbf{x}) \in \mathcal{U}$ that asymptotically drives the system to the optimal equilibrium point $(\mathbf{x}_f, \mathbf{u}_f)$. Finding this region of attraction corresponds to finding the largest region around the optimal equilibrium point with radius c_f in which the control law is stabilizing for the nonlinear system $\mathbf{x}_{k+1} = \mathbf{f}(\mathbf{x}_k, \mathbf{u}_k)$.

Consider the nonlinear system (1), split into linear and nonlinear parts,

$$\mathbf{x}_{k+1} = \mathbf{f}(\mathbf{x}_k, \mathbf{u}_k) = A\Delta\mathbf{x}_k + B\Delta\mathbf{u}_k + \phi(\Delta\mathbf{x}_k, \Delta\mathbf{u}_k) \tag{9}$$

where,

$$A = \left.\frac{\partial \mathbf{f}}{\partial \mathbf{x}}\right|_{(\mathbf{x}_f,\mathbf{u}_f)}, B = \left.\frac{\partial \mathbf{f}}{\partial \mathbf{u}}\right|_{(\mathbf{x}_f,\mathbf{u}_f)}$$

$\Delta\mathbf{x} := (\mathbf{x} - \mathbf{x}_f)$, $\Delta\mathbf{u} := (\mathbf{u} - \mathbf{u}_f)$ and $\phi(\Delta\mathbf{x}_k, \Delta\mathbf{u}_k)$ is the linearization error.

We propose to use an infinite horizon LQR applied on the linearized system as the stabilizing controller in the terminal region:

$$V_f(\mathbf{x}) \equiv \Delta\mathbf{x}^\mathsf{T} P \Delta\mathbf{x} = \min \sum_{k=0}^{\infty} \left(\Delta\mathbf{x}_k^\mathsf{T} Q \Delta\mathbf{x}_k + \Delta\mathbf{u}_k^\mathsf{T} R \Delta\mathbf{u}_k\right) \tag{10}$$

s.t.

$$\Delta\mathbf{x}_{k+1} = A\Delta\mathbf{x}_k + B\Delta\mathbf{u}_k, \quad \forall k = 0, \dots, \infty \tag{11}$$

where $P \succ 0$. By solving the discrete algebraic Riccati equation,

$$P = A^\mathsf{T} P A - (A^\mathsf{T} P B)(B^\mathsf{T} P B + R)^{-1}(B^\mathsf{T} P A) + Q \tag{12}$$

the LQR control law is given by,

$$\mathbf{u}_k = \kappa_f(\mathbf{x}_k) = \mathbf{u}_f - K(\mathbf{x}_k - \mathbf{x}_f) \tag{13}$$

with

$$K = (R + B^\mathsf{T} P B)^{-1} B^\mathsf{T} P A \tag{14}$$

The nonlinear system (1) controlled by the LQR control law (13) is then given by,

$$\Delta\mathbf{x}_{k+1} = A_{cl}\Delta\mathbf{x}_k + \overline{\phi}(\Delta\mathbf{x}_k) \tag{15}$$

where $A_{cl} = (A - BK)$ and $\overline{\phi}(\Delta\mathbf{x}_k) = \phi(\Delta\mathbf{x}_k, -K\Delta\mathbf{x}_k)$. In the LQR control design, we ignored the nonlinear effect $\phi(\Delta\mathbf{x}_k, \Delta\mathbf{u}_k)$. However, in order to show that the LQR controller stabilizes the nonlinear system, the linearization error must be bounded, which is formalized below.

Lemma 2 ([9]). *There exists $M, q \in \mathbb{R}_+$ such that*

$$|\overline{\phi}(\Delta\mathbf{x})| \leq M|\Delta\mathbf{x}|^q, \ \ \forall\mathbf{x} \in \mathcal{X} \tag{16}$$

Proof. See [9]. □

The radius of the terminal region of attraction to the optimal equilibrium point is given by (19), which depends on the bounds on the linearization error from Lemma 2. However, quantifying the bound analytically may be tedious as pointed out in [9]. Instead, the authors in [9] proposed to explicitly fit M and q in (16) via offline simulations, which will also be adopted in this paper. Here, we solve a series of one step simulations offline, using the LQR controller for several randomly sampled initial conditions from the state space. The linearization error is then quantified for all the simulations by subtracting the linear part of the system.

$$\phi(\Delta\mathbf{x}_k, \Delta\mathbf{u}_k) = \mathbf{f}(\Delta\mathbf{x}_k, -K\Delta\mathbf{x}_k) - A_{cl}\Delta\mathbf{x}_k \tag{17}$$

Note that this procedure is done only once, offline during the design of the controller.

Lemma 3. *There exists a region of attraction around the optimal equilibrium point* $\mathbf{x}_f$

$$\mathcal{X}_f := \{\mathbf{x} \mid |\mathbf{x} - \mathbf{x}_f| \leq c_f\} \tag{18}$$

such that the system controlled using a stabilizing LQR control law (13) in the interior of this region asymptotically converges to the optimal equilibrium point $\mathbf{x}_f$ *and the radius of the region of attraction is given by,*

$$c_f := \left(\frac{-\overline{\sigma}\Lambda + \sqrt{(\overline{\sigma}\Lambda)^2 + (\underline{\lambda}_W - \epsilon_{LQ})\Lambda}}{\Lambda M}\right)^{\frac{1}{q-1}} \tag{19}$$

where $\overline{\sigma}$ *is the maximum singular value of* A_{cl}*,* $\overline{\lambda}_W$ *and* $\underline{\lambda}_W$ *are the maximum and minimum eigenvalues of* $W := Q + K^{\mathsf{T}}RK$*,* $\Lambda := \frac{\overline{\lambda}_W}{(1-\overline{\sigma}^2)}$*, and* ϵ_{LQ} *is the margin for strong descent of* $V_f(\mathbf{x})$*.*

Proof. See [9]. □

Remark 1. Note that the stabilizing control law in the terminal region is designed such that it satisfies the control constraints, i.e. $\kappa_f(\mathbf{x}) \in \mathcal{U}$ for all $\mathbf{x} \in \mathcal{X}_f$. Consequently, $\mathcal{X}_f$ can be assumed to be control invariant under the control law $\mathbf{u} = \kappa_f(\mathbf{x})$.

With the existence of a region of attraction to the optimal equilibrium point, we can now design an adaptive horizon economic NMPC (AH-ENMPC) framework with a terminal cost and region, where the length of the prediction horizon $\tilde{N}_t \leq N$ at time t is chosen such that it is just enough to reach this terminal region $\mathcal{X}_f$. The adaptive horizon economic NMPC with prediction horizon length $\tilde{N}_t \leq N$ is then written as,

$$V_{\tilde{N}_t}(\hat{\mathbf{x}}_t) := \min_{\mathbf{x}_k, \mathbf{u}_k} V_f(\mathbf{x}_{\tilde{N}_t}) + \sum_{k=0}^{\tilde{N}_t-1} \ell(\mathbf{x}_k, \mathbf{u}_k) \tag{20a}$$

s.t.

$$\mathbf{x}_{k+1} = \mathbf{f}(\mathbf{x}_k, \mathbf{u}_k) \tag{20b}$$

$$\mathbf{x}_0 = \hat{\mathbf{x}}_t \tag{20c}$$

$$\mathbf{x}_k \in \mathcal{X}, \quad \mathbf{u}_k \in \mathcal{U} \tag{20d}$$

$$\mathbf{x}_{\tilde{N}_t} \in \mathcal{X}_f \tag{20e}$$

$$\forall k \in \{0, \dots, \tilde{N}_t - 1\}$$

Note that this formulation replaces the original economic NMPC (2), where the terminal penalty $V_f(\mathbf{x}_{\tilde{N}})$ is given by $(\mathbf{x}_{\tilde{N}} - \mathbf{x}_f)^{\mathsf{T}}P(\mathbf{x}_{\tilde{N}} - \mathbf{x}_f)$. This ensures that the state trajectory asymptotically converges to the optimal equilibrium point within the terminal region.

Remark 2. Since in the terminal region, the control law is designed such that the terminal penalty cost $V_f(\mathbf{x}_{\tilde{N}}) \equiv (\mathbf{x}_{\tilde{N}} - \mathbf{x}_f)^{\mathsf{T}}P(\mathbf{x}_{\tilde{N}} - \mathbf{x}_f)$ monotonically decreases [9], this may conflict with the economic objective $\ell(\cdot,\cdot)$ inside the terminal region. Hence, there may be a trade-off between the economic performance (small size of the terminal region) and the computation cost (large size of the terminal region). For this reason, the radius of the terminal region $\mathcal{X}_f$ may be chosen smaller than c_f, such that the economic loss due to enforcing a monotonically decreasing terminal region is negligible. Naturally all the desirable properties of the terminal region established in Lemma 3 still follow in this case, since $0 < \varepsilon \leq c_f$, where ε is the new radius of the terminal region.

Algorithm 1 details the offline steps involved in determining the terminal region and the cost-to-go approximation.

Algorithm 1 Offline algorithm to design the terminal region and the terminal cost function.

Define LQR tuning parameters Q and R.

$(\mathbf{x}_f, \mathbf{u}_f) \leftarrow$ solve steady-state optimization problem (7).
$A\Delta\mathbf{x}_k + B\Delta\mathbf{u}_k \leftarrow$ linearize nonlinear model (1) around $(\mathbf{x}_f, \mathbf{u}_f)$.
$P \leftarrow$ Solve discrete algebraic Riccati equation (12).
$\Delta\mathbf{x}_{k+1} \leftarrow$ one-step simulations with several random initial states $\mathbf{x}_k \in \mathcal{X}$.
$\phi \leftarrow \mathbf{f}(\mathbf{x}_k, \kappa(\mathbf{x}_k)) - A_{cl}(\mathbf{x}_k - \mathbf{x}_f)$ ▷ linearization error
Determine bounds on linearization error M, q using $|\phi|$
$c_f \leftarrow$ compute radius of the terminal region using (19)

Output: $\mathcal{X}_f$, P

The algorithm to determine the terminal region presented above is based on linearizing the system around the optimal equilibrium pair $(\mathbf{x}_f, \mathbf{u}_f)$. However, the optimal equilibrium pair depends on disturbances, and may change as the disturbances change. To reflect this, one can determine the radius of the terminal region c_f and the cost-to-go matrix P for different realizations and choose the smallest terminal region and the corresponding cost-to-go matrix. This would involve repeating Algorithm 1 for different disturbance realizations, which is performed once offline during the design of the controller.

4. Adaptive horizon economic NMPC (AH-ENMPC)

Now that we have presented a method to construct the terminal region $\mathcal{X}_f$, we now present an algorithm to choose the prediction horizon length $\tilde{N}$, which is sufficient to reach the terminal region. The first step is to determine a minimum horizon length N_{min} (typically chosen through simulation or domain knowledge). At the first time step $t = 0$ we initialize $\tilde{N}_0 = N$, which is the full horizon length. The prediction horizon length is defined to take an integer number from a bounded set $\mathcal{Z} := \{\tilde{N} | N_{min} \leq \tilde{N} \leq N, \tilde{N} \in \mathbb{Z}_+\}$. The maximum prediction horizon length N is chosen such that the economic NMPC problem is always feasible. The minimum length N_{min} is chosen via simulations such that the ENMPC problem is a good approximation of the infinite horizon problem [9].

The objective is to define a process $H : \mathbb{R}^{n_x} \times \mathbb{R}^{n_x} \times \mathcal{Z} \to \mathcal{Z}$ that determines the length of the prediction horizon to be used at time step $t+1$ based on the current state $\hat{\mathbf{x}}_t$, successor state[1] $\hat{\mathbf{x}}_{t+1|t}$, and the current horizon length $\tilde{N}_t$. One approach is to use

[1] Which denotes the states at time step $t+1$ predicted at time step t using $\hat{\mathbf{x}}_t$ and (1).

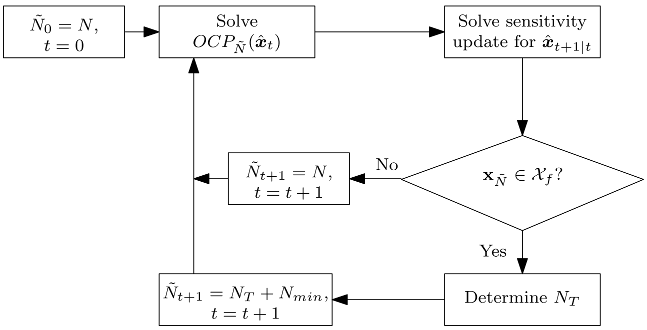

Fig. 1. Algorithm to determine the reduced horizon length $\tilde{N}$ starting from a sufficiently long horizon length N.

the NLP sensitivity update to determine the minimum horizon length required to reach the terminal region, which is described below.

At each time step t, we solve the economic NMPC problem $OCP_{\tilde{N}_t}(\hat{\mathbf{x}}_t)$ in Eq. (20). Using the NLP sensitivity, we then solve the parametric sensitivity problem with the initial condition $\hat{\mathbf{x}}_t$ as the parameter. Using the successor state $\hat{\mathbf{x}}_{t+1|t}$ as the parametric perturbation, we obtain the predicted state trajectory starting from $\hat{\mathbf{x}}_{t+1|t}$.

Let $\mathbf{s}^*(\hat{\mathbf{x}}_t)$ denote the combined primal–dual optimal solution of $OCP_{\tilde{N}_t}(\hat{\mathbf{x}}_t)$, and the active constraint gradients be linearly independent, then the parametric sensitivity provides the linearized approximation of the optimal solution with $\hat{\mathbf{x}}_{t+1|t}$ as the initial condition,

$$\mathbf{s}^*(\hat{\mathbf{x}}_{t+1|t}) \approx \mathbf{s}^*(\hat{\mathbf{x}}_t) + \frac{\partial \mathbf{s}^*(\hat{\mathbf{x}}_t)^T}{\partial \hat{\mathbf{x}}_t}(\hat{\mathbf{x}}_{t+1|t} - \hat{\mathbf{x}}_t) \tag{21}$$

For the sake of brevity, the parametric sensitivity update step and how to compute $\frac{\partial \mathbf{s}^*(\hat{\mathbf{x}}_t)}{\partial \hat{\mathbf{x}}_t}$ is detailed in the Appendix.

From the predicted state trajectory provided by the sensitivity update $\mathbf{s}^*(\hat{\mathbf{x}}_{t+1|t})$ we can determine the number of time steps N_T required to reach the terminal region $\mathcal{X}_f$. At time step $t+1$, we can then set the horizon length $\tilde{N}_{t+1} = N_T + N_{min}$. However, if the state trajectory from the sensitivity update starting from $\hat{\mathbf{x}}_{t+1|t}$ does not reach the terminal region, then at time step $t+1$ we set the full horizon length $\tilde{N}_{t+1} = N$.

To summarize, at each time step, this involves solving the NLP problem with $\tilde{N}_t$ prediction horizon length and solving the sensitivity problem. The prediction horizon length is updated online based on the one-step ahead sensitivity predictions along with a minimum number of samples N_{min} added as a safety factor. The sketch of the adaptive horizon algorithm is shown in Algorithm 2 and schematically represented in Fig. 1.

Remark 3. We assume that the OCP (20) at time t is always feasible for $\tilde{N}_t = N$. The process H (now defined by Algorithm 2) is designed such that if the OCP (20) with horizon length $\tilde{N}_t$ is feasible at time t, then it is also feasible at time $t+1$ with horizon length $\tilde{N}_{t+1}$. Although N_T in Algorithm 2 is determined based on NLP sensitivity update, the safety factor N_{min} can be chosen such that the terminal region is $\tilde{N}_{t+1}$ reachable. This can be done using offline simulations, since finding N_{min} that rigorously guarantees this assumption may in general be difficult, and is not the focus of this paper.

5. Stability properties of the AH-ENMPC

In this section, we study the stability properties of the adaptive horizon economic NMPC framework presented in Section 4.

Algorithm 2 Sensitivity-based adaptive horizon algorithm.

Define full horizon length N, minimum length N_{min}.
Determine terminal region $\mathcal{X}_f$ and cost-to-go approximation using Algorithm 1.
Initialize $\tilde{N}_0 = N$.

Input: at each time step t: initial state $\hat{\mathbf{x}}_t$

$\mathbf{s}^*(\hat{\mathbf{x}}_t) \leftarrow$ Solve $OCP_{\tilde{N}_t}(\hat{\mathbf{x}}_t)$
One-step ahead prediction $\hat{\mathbf{x}}_{t+1|t} \leftarrow \mathbf{f}(\hat{\mathbf{x}}_t, \boldsymbol{\mu}_t)$
$\mathbf{s}^*(\hat{\mathbf{x}}_{t+1|t}) \leftarrow$ Solve the sensitivity problem (21) that approximates $OCP_{\tilde{N}_t}(\hat{\mathbf{x}}_{t+1|t})$.
Obtain state trajectory $\mathbf{x}_{\tilde{N}_t}$ from $\mathbf{s}^*(\hat{\mathbf{x}}_{t+1|t})$
if $\mathbf{x}_{\tilde{N}_t} \in \mathcal{X}_f$ **then**
  Determine N_T, step at which $\mathcal{X}_f$ is reached.
  Set $\tilde{N}_{t+1} \leftarrow N_T + N_{min}$
else
  Set $\tilde{N}_{t+1} \leftarrow N$
end if
$t \leftarrow t+1$

Output: $\mathbf{s}^*(\hat{\mathbf{x}}_t)$, $\tilde{N}_{t+1}$

We follow the Lyapunov stability framework where we want to ensure the existence of a Lyapunov function,

$$\begin{aligned} V_{\tilde{N}_{t+1}}(\hat{\mathbf{x}}_{t+1}) - V_{\tilde{N}_t}(\hat{\mathbf{x}}_t) \le & \sum_{k=1}^{\tilde{N}_{t+1}} \ell(\mathbf{x}_k, \mathbf{u}_k) + V_f(\mathbf{x}_{\tilde{N}_{t+1}+1}) \\ & - \sum_{k=0}^{\tilde{N}_t - 1} \ell(\mathbf{x}_k, \mathbf{u}_k) - V_f(\mathbf{x}_{\tilde{N}_t}) \end{aligned} \tag{22}$$

However, for economic NMPC problems, the economic stage cost $\ell(\mathbf{x}_k, \mathbf{u}_k)$ may not be a $\mathcal{K}$ function of $\mathbf{x}_k$, and can take any arbitrary form. In general, the local minima are not guaranteed to be the global minima and in this case, the right hand side of the inequality (22) may not always be negative. Therefore, the objective function of the economic NMPC cannot be directly used as a Lyapunov function and we need additional properties.

For economic NMPC problems, dissipativity as defined in Definitions 5 and 6 can be used to establish stability.

As established in [13], the dissipativity condition is satisfied if the economic stage cost $\ell(\cdot,\cdot)$ and the system (1) form a strongly dual problem. If the steady-state optimization problem has a strongly convex Lagrange function, then this leads to strong duality [18]. This leads to the idea of rotated stage costs given by

$$\psi(\mathbf{x}, \mathbf{u}) := \ell(\mathbf{x}, \mathbf{u}) + \lambda(\mathbf{x}) - \lambda(\mathbf{f}(\mathbf{x}, \mathbf{u})) \tag{23}$$

Similarly, the rotated terminal cost

$$\Psi(\mathbf{x}_{\tilde{N}}) := V_f(\mathbf{x}_{\tilde{N}}) + \lambda(\mathbf{x}_{\tilde{N}}) \tag{24}$$

can be formed.

As shown in [19, Lemma 9], the existence of a stabilizing control law $\mathbf{u} = \kappa_f(\mathbf{x})$ in the terminal region and the control invariance property of $\mathcal{X}_f$ (cf. Remark 1) implies that the rotated terminal cost satisfies

$$\Psi(\mathbf{x}_{N+1}) - \Psi(\mathbf{x}_N) \le -\psi(\mathbf{x}_N, \mathbf{u}_N) + \ell(\mathbf{x}_f, \mathbf{u}_f) \qquad \forall \mathbf{x}_N \in \mathcal{X}_f \tag{25}$$

where $\mathbf{u}_N = \kappa_f(\mathbf{x}_f)$ is given by the stabilizing control law (13).

Considering the rotated stage cost (23) and terminal cost (24), the OCP (20) can be rewritten as,

$$\widehat{V}_{\tilde{N}}(\hat{\mathbf{x}}_t) := \min_{\mathbf{x}_k,\mathbf{u}_k} \Psi(\mathbf{x}_{\tilde{N}}) + \sum_{k=0}^{\tilde{N}-1} \psi(\mathbf{x}_k, \mathbf{u}_k) \quad \text{s.t. (20b)–(20e)} \tag{26}$$

Lemma 4 (*Rotation Does Not Alter Optimal Solution [15]*)**.** *If the adaptive horizon ENMPC solved with the stage cost $\ell(\mathbf{x}, \mathbf{u})$ and terminal cost $V_f(\mathbf{x}_{\tilde{N}})$, admits an optimal solution $\mathbf{u}^*(\cdot, \hat{\mathbf{x}}_t)$ for any $\hat{\mathbf{x}}_t \in \mathcal{X}$, then for the same horizon length and initial condition, the optimal solution $\mathbf{u}^*(\cdot, \hat{\mathbf{x}}_t)$ is also optimal for the AH-ENMPC solved with rotated stage cost $\psi(\mathbf{x}, \mathbf{u})$ and terminal cost $\Psi(\mathbf{x}_{\tilde{N}})$.*

Proof. Expanding the rotated cost function (26) gives

$$\widehat{V}_{\tilde{N}}(\hat{\mathbf{x}}_t) = \Psi(\mathbf{x}_{\tilde{N}}) + \sum_{k=0}^{\tilde{N}-1} \psi(\mathbf{x}_k, \mathbf{u}_k) \tag{27a}$$

$$= \sum_{k=0}^{\tilde{N}-1} [\ell(\mathbf{x}_k, \mathbf{u}_k) + \lambda(\mathbf{x}_k) - \lambda(\mathbf{x}_{k+1})] + V_f(\mathbf{x}_{\tilde{N}}) - \lambda(\mathbf{x}_{\tilde{N}}) \tag{27b}$$

$$= \sum_{k=0}^{\tilde{N}-1} \ell(\mathbf{x}_k, \mathbf{u}_k) + V_f(\mathbf{x}_{\tilde{N}}) + \lambda(\mathbf{x}_0) = V_{\tilde{N}}(\hat{\mathbf{x}}_t) + \lambda(\hat{\mathbf{x}}_t) \tag{27c}$$

which differs from the original cost only by the constant term $\lambda(\hat{\mathbf{x}}_t)$. □

This implies that the optimal solution for the OCP (26) is identical to (20). Therefore, one can equivalently analyze the stability of (26).

If (23) is strongly convex, then strong duality can be guaranteed. However, if these are not strongly convex functions, then a simple approach to ensure strong convexity of (23) is by adding regularization terms

$$\frac{1}{2}|(\mathbf{x} - \mathbf{x}_f, \mathbf{u} - \mathbf{u}_f)|^2_{\hat{Q}} \tag{28}$$

where $\hat{Q}$ is a suitably defined regularization weighting matrix, such that the resulting regularized rotated stage cost function is strongly convex. The regularized rotated stage cost is given as,

$$\psi_{reg}(\mathbf{x}, \mathbf{u}) := \psi(\mathbf{x}, \mathbf{u}) + \frac{1}{2}|(\mathbf{x} - \mathbf{x}_f, \mathbf{u} - \mathbf{u}_f)|^2_{\hat{Q}} \tag{29}$$

At the optimum,

$$\nabla \psi_{reg} = \nabla \psi = 0 \tag{30a}$$

$$\nabla^2 \psi_{reg} = \nabla^2 \psi + \hat{Q} \tag{30b}$$

To ensure strong convexity, one must have $\nabla^2 \psi_{reg} \succ 0, \forall (\mathbf{x}, \mathbf{u}) \in \mathcal{X} \times \mathcal{U}$. Therefore, $\hat{Q}$ must be chosen such that the eigenvalues of $(\nabla^2 \psi + \hat{Q}) > 0$ over the entire feasible set $\mathcal{X} \times \mathcal{U}$. For example, the regularization weighting matrix can be determined by applying the Gresgorin's theorem to find the minimal regularization matrix that makes the regularized rotated stage cost strongly convex as explained in [20]. However, it is worth noting that the regularization with $\hat{Q}$ could make (28) a conservative, sluggish controller. An alternative approach to adding regularization terms, may be to impose a constraint that enforces a descent condition on a tracking Lyapunov function as shown in [21, Section 4.2].

Consider the rotated cost evaluated using the stabilizing control law $\mathbf{u}_k = \kappa_f(\mathbf{x}_k)$,

$$\widehat{V}^{\kappa}_{\tilde{N}}(\hat{\mathbf{x}}_t) := \Psi(\mathbf{x}_{\tilde{N}}) + \sum_{k=0}^{\tilde{N}-1} \psi(\mathbf{x}_k, \kappa_f(\mathbf{x}_k))$$

Lemma 5. *There exists $\alpha_1 \in \mathcal{K}_\infty$ such that $|\widehat{V}^{\kappa}_{\tilde{N}}(\mathbf{x}) - \Psi(\mathbf{x})| \le \alpha_1(|\mathbf{x} - \mathbf{x}_f|)$ for all $\hat{\mathbf{x}}_t \in \mathcal{X}_f$ and $\alpha_2 \in \mathcal{K}_\infty$ such that $|\Psi(\hat{\mathbf{x}}_t) - \widehat{V}_N(\hat{\mathbf{x}}_t)| \le \alpha_2(|\mathbf{x} - \mathbf{x}_f|)$ for all $\hat{\mathbf{x}}_t \in \mathcal{X}_f$.*

Proof. See [9]. □

Assumption 5. The solution of the AH-ENMPC (20) with horizon length $\tilde{N}_t \ge N_{min}$ satisfies

$$\alpha_1(|\mathbf{x}_{\tilde{N}_t} - \mathbf{x}_f|) - \alpha_l(|\mathbf{x}_0 - \mathbf{x}_f|) \le -\alpha'_l(|\mathbf{x}_0 - \mathbf{x}_f|) \text{ if } \tilde{N}_{t+1} > \tilde{N}_t$$

$$\alpha_2(|\mathbf{x}_{\tilde{N}_{t+1}+1} - \mathbf{x}_f|) - \alpha_l(|\mathbf{x}_0 - \mathbf{x}_f|) \le -\alpha'_l(|\mathbf{x}_0 - \mathbf{x}_f|) \text{ if } \tilde{N}_{t+1} < \tilde{N}_t$$

This essentially means that the approximation error using a stabilizing control law in the terminal region must be negligible (cf. Remark 2). This assumption can be enforced using a sufficiently large N_{min} which is selected through simulations as explained in [9].

Theorem 1 (*Nominal Stability of AH-ENMPC*)**.** *Consider the adaptive horizon economic NMPC problem (20) applied to the system (1). Given Assumptions 1, 4, and 5, the closed-loop system is asymptotically stable at $\mathbf{x}_f$.*

Proof. According to Lemma 4, since the optimal solutions coincide, we can consider the rotated stage and terminal cost in the economic NMPC. First we show that rotated cost function $\widehat{V}_{\tilde{N}}(\hat{\mathbf{x}}_t)$ is a suitable Lyapunov function for the closed-loop system by considering the case where $\tilde{N}_{t+1} = \tilde{N}_t = \tilde{N}$.

$$\begin{aligned}
&\widehat{V}_{\tilde{N}}(\hat{\mathbf{x}}_{t+1}) - \widehat{V}_{\tilde{N}}(\hat{\mathbf{x}}_t) \\
&= \sum_{k=1}^{\tilde{N}} \psi(\mathbf{x}_k, \mathbf{u}_k) + \Psi(\mathbf{x}_{\tilde{N}+1}) - \sum_{k=0}^{\tilde{N}-1} \psi(\mathbf{x}_k, \mathbf{u}_k) - \Psi(\mathbf{x}_{\tilde{N}}) \\
&= \psi(\mathbf{x}_{\tilde{N}}, \mathbf{u}_{\tilde{N}}) - \psi(\mathbf{x}_0, \mathbf{u}_0) + \Psi(\mathbf{x}_{\tilde{N}+1}) - \Psi(\mathbf{x}_{\tilde{N}})
\end{aligned}$$

From (25), we have

$$\widehat{V}_{\tilde{N}}(\hat{\mathbf{x}}_{t+1}) - \widehat{V}_{\tilde{N}}(\hat{\mathbf{x}}_t) \le \ell(\mathbf{x}_f, \mathbf{u}_f) - \psi(\mathbf{x}_0, \mathbf{u}_0)$$

From the definition of the rotated stage cost (23) and strict dissipativity (6),

$$\begin{aligned}
&\widehat{V}_{\tilde{N}}(\hat{\mathbf{x}}_{t+1}) - \widehat{V}_{\tilde{N}}(\hat{\mathbf{x}}_t) \\
&\le \ell(\mathbf{x}_f, \mathbf{u}_f) - \ell(\mathbf{x}_0, \mathbf{u}_0) - \lambda(\mathbf{x}_0) + \lambda(\mathbf{f}(\mathbf{x}_0, \mathbf{u}_0)) \\
&\le -\alpha_l(|\mathbf{x}_0 - \mathbf{x}_f|)
\end{aligned}$$

where $\mathbf{x}_0 = \hat{\mathbf{x}}_t$ and $\mathbf{u}_0 = \boldsymbol{\mu}_t(\hat{\mathbf{x}}_t)$. Hence $\widehat{V}_{\tilde{N}}(\hat{\mathbf{x}}_t)$ is a Lyapunov function and $\mathbf{x}_f$ is an asymptotically stable equilibrium point of the closed loop system. Now we can use the same framework and consider the case where $\tilde{N}_{t+1} \ne \tilde{N}_t$.

Consider the case with increasing horizon length $\tilde{N}_{t+1} > \tilde{N}_t$. The candidate Lyapunov function is given by,

$$\begin{aligned}
&\widehat{V}_{\tilde{N}_{t+1}}(\hat{\mathbf{x}}_{t+1}) - \widehat{V}_{\tilde{N}_t}(\hat{\mathbf{x}}_t) \\
&= \sum_{k=1}^{\tilde{N}_{t+1}} \psi(\mathbf{x}_k, \mathbf{u}_k) + \Psi(\mathbf{x}_{\tilde{N}_{t+1}+1}) - \sum_{k=0}^{\tilde{N}_t-1} \psi(\mathbf{x}_k, \mathbf{u}_k) - \Psi(\mathbf{x}_{\tilde{N}_t}) \\
&= \sum_{k=1}^{\tilde{N}_t-1} \psi(\mathbf{x}_k, \mathbf{u}_k) + \sum_{k=\tilde{N}_t}^{\tilde{N}_{t+1}} \psi(\mathbf{x}_k, \mathbf{u}_k) + \Psi(\mathbf{x}_{\tilde{N}_{t+1}+1}) \\
&\quad - \psi(\mathbf{x}_0, \mathbf{u}_0) - \sum_{k=1}^{\tilde{N}_t-1} \psi(\mathbf{x}_k, \mathbf{u}_k) - \Psi(\mathbf{x}_{\tilde{N}_t}) \\
&= -\psi(\mathbf{x}_0, \mathbf{u}_0) + \sum_{k=\tilde{N}_t}^{\tilde{N}_{t+1}} \psi(\mathbf{x}_k, \mathbf{u}_k) + \Psi(\mathbf{x}_{\tilde{N}_{t+1}+1}) - \Psi(\mathbf{x}_{\tilde{N}_t})
\end{aligned}$$

$$= -\psi(\mathbf{x}_0, \mathbf{u}_0) + \widehat{V}^{\kappa}_{\tilde{N}_{t+1}+1-\tilde{N}_t}(\mathbf{x}_{\tilde{N}_t}) - \Psi(\mathbf{x}_{\tilde{N}_t})$$
$$\leq -\alpha_l(|\mathbf{x}_0 - \mathbf{x}_f|) + \alpha_1(|\mathbf{x}_{\tilde{N}_t} - \mathbf{x}_f|) \leq -\alpha_l'(|\mathbf{x}_0 - \mathbf{x}_f|)$$

Now consider the case with decreasing horizon length $\tilde{N}_{t+1} < \tilde{N}_t$. The candidate Lyapunov function is given by,

$$\widehat{V}_{\tilde{N}_{t+1}}(\hat{\mathbf{x}}_{t+1}) - \widehat{V}_{\tilde{N}_t}(\hat{\mathbf{x}}_t)$$
$$= \sum_{k=1}^{\tilde{N}_{t+1}} \psi(\mathbf{x}_k, \mathbf{u}_k) + \Psi(\mathbf{x}_{\tilde{N}_{t+1}+1}) - \sum_{k=0}^{\tilde{N}_t-1} \psi(\mathbf{x}_k, \mathbf{u}_k) - \Psi(\mathbf{x}_{\tilde{N}_t})$$
$$= \sum_{k=1}^{\tilde{N}_{t+1}} \psi(\mathbf{x}_k, \mathbf{u}_k) + \Psi(\mathbf{x}_{\tilde{N}_{t+1}+1}) - \Psi(\mathbf{x}_{\tilde{N}_t})$$
$$- \psi(\mathbf{x}_0, \mathbf{u}_0) - \sum_{k=1}^{\tilde{N}_{t+1}} \psi(\mathbf{x}_k, \mathbf{u}_k) - \sum_{k=N_{t+1}+1}^{\tilde{N}_t-1} \psi(\mathbf{x}_k, \mathbf{u}_k)$$
$$= -\psi(\mathbf{x}_0, \mathbf{u}_0) + \Psi(\mathbf{x}_{\tilde{N}_{t+1}+1}) - \sum_{k=N_{t+1}+1}^{\tilde{N}_t-1} \psi(\mathbf{x}_k, \mathbf{u}_k) - \Psi(\mathbf{x}_{\tilde{N}_t})$$
$$= -\psi(\mathbf{x}_0, \mathbf{u}_0) + \Psi(\mathbf{x}_{\tilde{N}_{t+1}+1}) - \widehat{V}_{\tilde{N}_t-\tilde{N}_{t+1}+1}(\mathbf{x}_{\tilde{N}_{t+1}+1})$$
$$\leq -\alpha_l(|\mathbf{x}_0 - \mathbf{x}_f|) + \alpha_2(|\mathbf{x}_{\tilde{N}_{t+1}+1} - \mathbf{x}_f|) \leq -\alpha_l'(|\mathbf{x}_0 - \mathbf{x}_f|)$$

Hence $\widehat{V}_{\tilde{N}}(\hat{\mathbf{x}}_t)$ is a Lyapunov function and the AH-ENMPC is asymptotically stable. □

Remark 4. As noted in [15] the rotation of the stage and terminal cost is not necessary for the implementation of the adaptive horizon economic NMPC, but is only needed to show stability properties.

6. Simulation example 1 — CSTR

In this section, we illustrate the concepts described above using a CSTR case example from [22], with a reversible exothermic reaction $A \rightleftharpoons B$. The objective is to maximize the product concentration C_B while penalizing the utility cost of heating the input stream using the inlet temperature $\mathbf{u} = T_i$ as the manipulated variable.

$$\min_{T_i} \ell = -[2.009C_B - (1.657 \times 10^{-3}(T_i - 410))^2]$$
$$s.t. \tag{31}$$
$$\frac{dC_A}{dt} = \frac{1}{\tau}(C_{A,i} - C_A) - r \tag{32}$$
$$\frac{dC_B}{dt} = \frac{1}{\tau}(C_{B,i} - C_B) + r \tag{33}$$
$$\frac{dT}{dt} = \frac{1}{\tau}(T_i - T) + \frac{-\Delta H_{rx}}{\rho C_p} r \tag{34}$$

where the concentrations in [mol/l] of the two components in the reactor are denoted by C_A and C_B, respectively. $C_{A,i}$ and $C_{B,i}$ denote the feed concentrations. T_i and T are the inlet and reaction temperatures, respectively and the reaction rate is given as $r = k_1C_A - k_2C_B$ with $k_1 = C_1 e^{\frac{-E_1}{RT}}$ and $k_2 = C_2 e^{\frac{-E_2}{RT}}$. The system has $n_x = 3$ states and $n_u = 1$ control input.

To ensure dissipativity and strong convexity, we add the regularization terms $\frac{1}{2}[q_A(C_A - C_A^*)^2 + q_B(C_B - C_B^*)^2 + q_T(T - T^*)^2 + q_{T_i}(T_i - T_i^*)^2]$ to the stage cost with $q_A = 27$, $q_B = 26$ and $q_T = q_{T_i} = 0$, which were chosen such that the eigenvalues of $(\nabla^2\psi + \hat{Q}) > 0$.

6.1. Terminal region calculation

To compute a terminal region, we design a LQR control law with $Q = 10$ and $R = 1$. As mentioned earlier, the linearization error bounds are quantified by explicitly fitting M and q in (16) via several one-step simulations offline. To quantify the linearization error in this example, we perform 10 000 such simulations offline, with random initial states. Here $M = 100\,000$ and $q = 2$ were found to be reasonable bounds as shown in Fig. 2 (orange line). Using (19), the radius of the terminal region is computed as $c_f = 1.2951 \times 10^{-6}$.

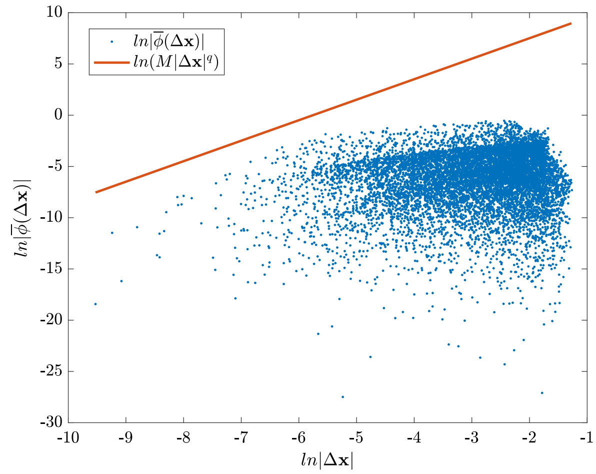

Fig. 2. Example 1: Nonlinearity bounds computed using 10 000 simulations.

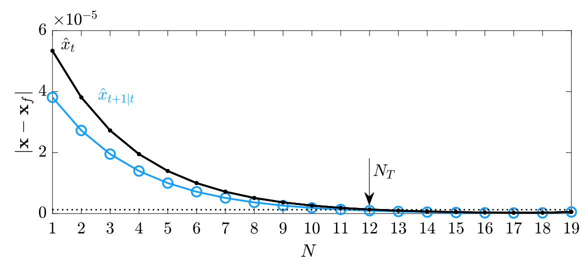

Fig. 3. Example1: Open-loop predicted optimal trajectory of $|\mathbf{x} - \mathbf{x}_f|$ at $t = 16$ (black) and the sensitivity update starting from the successor state (blue). (For interpretation of the references to color in this figure legend, the reader is referred to the web version of this article.)

6.2. Simulation results

The system was simulated with a sampling time of 10 s. The process was simulated for a total duration of 20 min. The proposed adaptive horizon economic NMPC controller with reduced horizon updated online (denoted by AH-ENMPC) was benchmarked against the economic NMPC with the full horizon length of $N = 60$ (denoted by ENMPC). $\tilde{N}_{min} = 3$ was chosen as the minimum length for the AH-ENMPC scheme. The controller was implemented using `CasADi v.3.4.5`[23] using `MATLAB` interface. The NLP was solved with `IPOPT` [24] using `MUMPS` linear solver on a 2.6 GHz Intel Core-i7 with 16 GB memory.

Fig. 3 shows the open-loop predicted optimal trajectory of $|\mathbf{x} - \mathbf{x}_f|$ at $t = 16$ in black. The sensitivity update (21) using the successor state $\hat{\mathbf{x}}_{t+1|t}$ is also shown in the same figure in blue. As described in Algorithm 2, the number of samples required to reach the terminal region N_T is determined using the sensitivity update, which is then used as the horizon length at the next time step with an additional safety factor of N_{min}.

Fig. 4 shows the open loop cost at time step $t = 30$, where it can be seen that the open loop optimal trajectory of the adaptive horizon economic NMPC with $\tilde{N} = 25$ samples is also admissible for the full horizon economic NMPC up to $N = 25$.

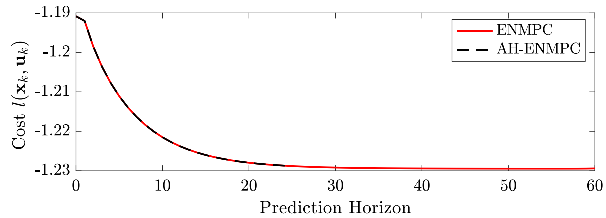

Fig. 4. Example1: Open loop predictions showing the stage cost at time step $t = 30$ for the adaptive horizon economic NMPC and the standard fixed horizon economic NMPC.

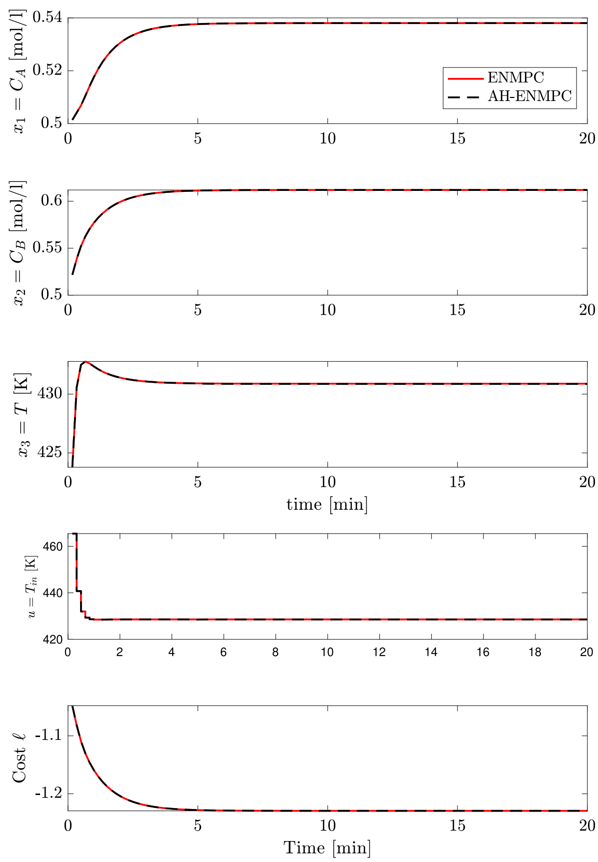

Fig. 5. Example 1 no noise case: Simulation results comparing the adaptive horizon economic NMPC with the standard fixed horizon economic NMPC.

Simulation without noise. Fig. 5 shows the closed-loop simulation results of the AH-ENMPC (dashed) and the standard ENMPC (solid) without measurement noise. It can be clearly seen that the performance of both the controllers are nearly identical. The only difference between the two controllers are the length of the prediction horizon. The standard economic NMPC had a fixed length of 60 samples, whereas the prediction horizon was updated online using Algorithm 2 for the adaptive horizon economic NMPC. The prediction horizon lengths and the corresponding CPU times are shown in Fig. 6. The average computation time and the total cumulative cost of the two approaches are also summarized in Table 1, which clearly shows that identical performance as the standard economic NMPC can be achieved with significantly less computation time by using the proposed adaptive horizon economic NMPC.

Simulation with noise. Fig. 7 shows the closed-loop simulation results of the AH-ENMPC (dashed) and the standard ENMPC (solid)

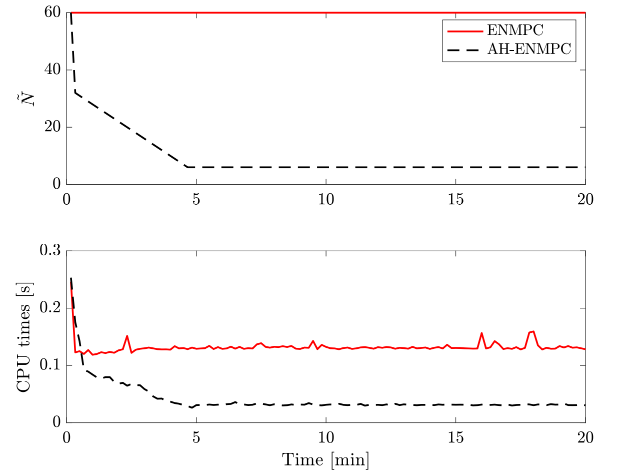

Fig. 6. Example 1 no noise case: Simulation results comparing the length of the prediction horizon and CPU time.

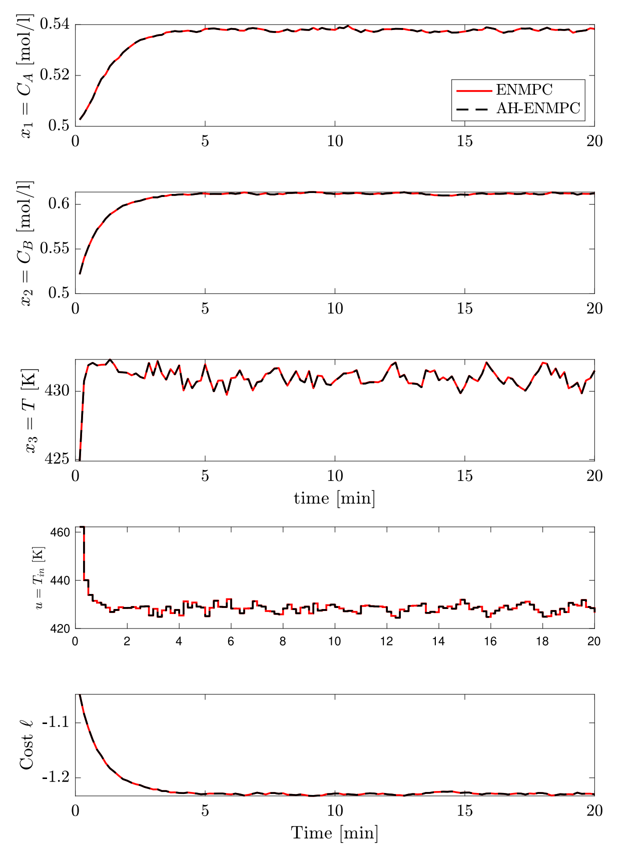

Fig. 7. Example 1 with noise case: Simulation results comparing the adaptive horizon economic NMPC with the standard fixed horizon economic NMPC.

with added measurement noise of zero mean and standard deviation $\sigma_i = [0.0005, 0.0005, 0.05]$. Again, it can be clearly seen that the performance of both the controllers are nearly identical. The prediction horizon lengths and the corresponding CPU times are shown in Fig. 6. The average computation time and the total cumulative cost of the two approaches are also summarized in Table 1, which clearly shows that identical performance as the standard economic NMPC can be achieved with significantly less computation time by using the proposed adaptive horizon economic NMPC (see Fig. 8).

Table 1
Example 1: Average computation time and cumulative cost for ENMPC and AH-ENMPC.

	No noise		With noise	
	Cumulative cost $\sum \ell[\$]$	Average CPU time [s]	Cumulative cost $\sum \ell[\$]$	Average CPU time [s]
ENMPC ($N = 60$)	−146.4480	0.1320	−146.4769	0.1580
AH-ENMPC	−146.4477	0.0307	−146.4767	0.0325

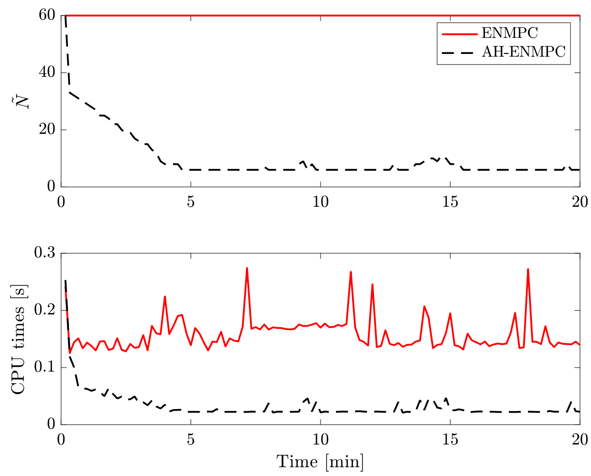

Fig. 8. Example 1 with noise case: Simulation results comparing the length of the prediction horizon and CPU time.

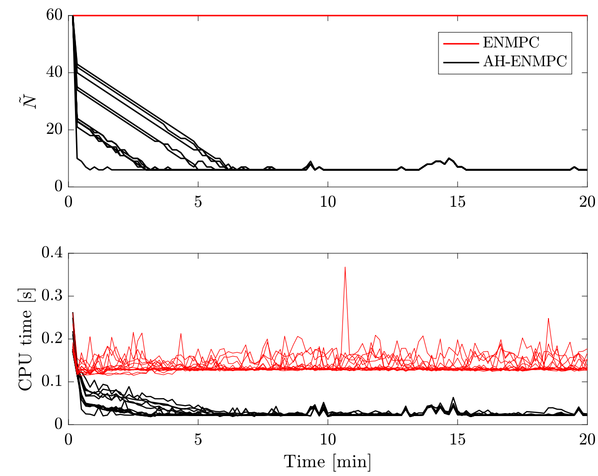

Fig. 9. Example 1 with noise case: Simulation results comparing the length of the prediction horizon and CPU time for 15 different simulation runs starting from different initial conditions $\hat{\mathbf{x}}_0$.

Simulation with different initial conditions. - We now perform the same simulation as above, but start with different initial conditions $\hat{\mathbf{x}}_0$ and compare the performance of the proposed AH-ENMPC scheme with the fixed horizon ENMPC. Fig. 9 (top subplot) shows the minimum horizon length required to reach the terminal region for 15 randomly chosen initial states. This plot clearly shows that for some initial conditions, the terminal region is reachable with a relatively short prediction horizon, whereas for some other initial conditions, longer prediction horizon is required. In other words, the minimum prediction horizon length required to reach the terminal region varies with the initial condition and is typically not known in advance. This is one of the main reasons why the prediction horizon of the MPC is chosen to be conservatively long in many practical applications, and further motivates the need for an adaptive horizon framework. The proposed AH-ENMPC scheme on the other hand, is able to determine and update the minimum prediction horizon length required to reach the terminal region in each simulation run.

The CPU time for the different simulation runs using ENMPC and the AH-ENMPC are also shown in Fig. 9 (bottom subplot). The average CPU time over the different simulation runs using the proposed AH-ENMPC was 0.0305 s, as opposed to 0.1374 s using ENMPC, which shows a 78% decrease in the average CPU time using the proposed AH-ENMPC scheme.

7. Simulation example 2 — Williams–Otto reactor

In this section, we now demonstrate the proposed AH-ENMPC scheme using a benchmark Williams–Otto reactor from [25]. Williams–Otto reactor is fed with two input streams F_A and F_B of pure components A and B, respectively to produce the products P and E, through the following set of chemical reactions,

$$A + B \rightarrow C$$
$$B + C \rightarrow P + E$$
$$C + P \rightarrow G$$

Feed stream $F_A = 1.8275$ kg/s is fixed, and the process is controlled using feed stream F_B and the reactor temperature T_R. The economic optimization problem is given by,

$$\begin{aligned} \min_{F_B, T_R} \ & \ell = -1043.38 x_P (F_A + F_B) + 20.92 x_E (F_A + F_B) \\ & \quad - 79.23 F_A - 118.34 F_B \\ \text{s.t.} \ & \mathbf{x} = \mathbf{f}(\mathbf{x}, \mathbf{u}) \\ & x_G \le 0.08 \end{aligned}$$

where x_i denotes the mass fraction of the ith component. The process has $n_x = 6$ states and $n_u = 2$ inputs. To ensure strong convexity, we add regularization terms $0.5|\mathbf{x} - \mathbf{x}_f|_{\hat{Q}}$ to the stage cost, with $\hat{Q} = 0.1 I_{6\times6}$, which was chosen to ensure that the eigenvalues of $(\nabla^2 \psi + \hat{Q}) > 0$. The terminal region was computed by quantifying the linearization error bounds by explicitly fitting M and q in (16) via several one-step simulations offline. To quantify the linearization error in this example, we perform 3 025 000 such simulations. Here $M = 1$ and $q = 2$ were found to be reasonable bounds as shown in Fig. 10 (orange line). This leads to a terminal region of attraction with radius $c_f = 5.6162 \times 10^{-4}$.

The system was simulated with a sampling time of 1min, with the nominal prediction horizon of $N = 60$ samples. Note that, in this example, although the terminal region was reachable with a shorter prediction horizon, this led to poor closed-loop performance. Therefore, we choose a prediction horizon of $N = 60$ to get the desired closed-loop performance, and then use the proposed AH-ENMPC scheme to reduce the computational delay. $\tilde{N}_{min} = 12$ was chosen as the minimum length of the prediction horizon in the AH-ENMPC scheme. The process was simulated for a total time of 60 min.

Fig. 11 shows the closed-loop simulation results of the AH-ENMPC (dashed) and the standard ENMPC (solid) with measurement noise of zero mean and standard deviation $\sigma_i = 5 \times 10^{-5}$. Again, it can be clearly seen that the performance of both the

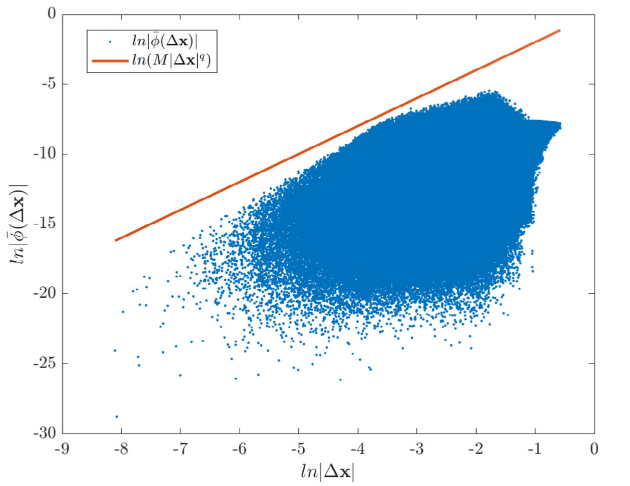

Fig. 10. Example 2: Nonlinearity bounds computed using 3 025 000 simulations.

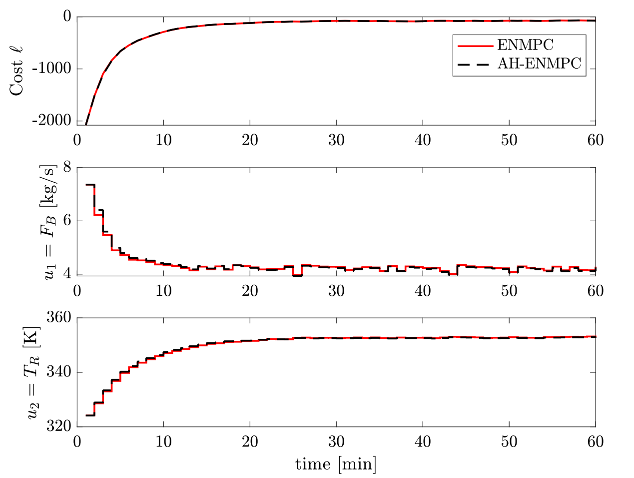

Fig. 11. Example 2 with noise: Simulation results comparing the adaptive horizon economic NMPC with the standard fixed horizon economic NMPC.

Table 2
Example 2: Average computation time and cumulative cost for ENMPC and AH-ENMPC.

	Cumulative cost $\sum \ell[\$]$	Average CPU time [s]
ENMPC	-2.578×10^4	0.4195
AH-ENMPC	-2.579×10^4	0.1421

controllers are nearly identical. The prediction horizon lengths and the corresponding CPU times are shown in Fig. 12. The average computation time and the total cumulative cost of the two approaches are also summarized in Table 2, which clearly shows that nearly identical performance as the standard economic NMPC can be achieved with significantly less computation time by using the proposed adaptive horizon economic NMPC.

8. Conclusion

This paper presents an adaptive horizon economic NMPC framework where we showed that we can reduce the computational delay by choosing a smaller prediction horizon length. We develop an approach to compute a terminal region to the optimal equilibrium point and show that the online optimization problem only needs to re-compute the optimal solution to this terminal region. We also showed that the proposed adaptive horizon economic NMPC is nominally stable. Simulation results demonstrate the effectiveness of the proposed approach. Extending this approach to more general economic NMPC formulations is a natural progression of this work. Explicit treatment of uncertainty and model mismatch in the proposed AH-ENMPC scheme would be another future research direction.

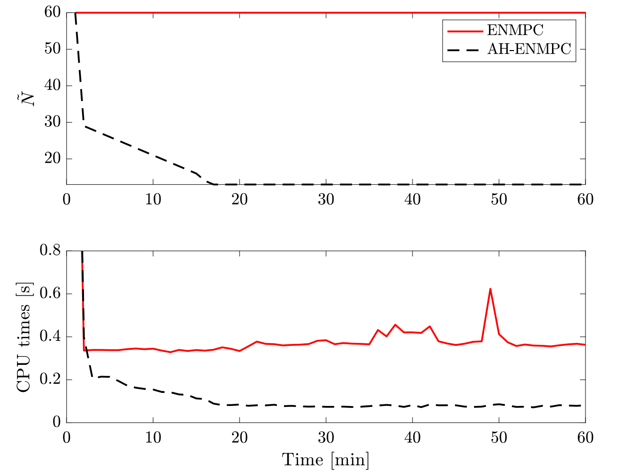

Fig. 12. Example 2 with noise: Simulation results comparing the length of the prediction horizon and CPU time.

CRediT authorship contribution statement

Dinesh Krishnamoorthy: Writing - original draft, Software, Conceptualization, Methodology. **Lorenz T. Biegler:** Conceptualization, Methodology, Writing - review & editing. **Johannes Jäschke:** Conceptualization, Methodology, Writing - review & editing.

Declaration of competing interest

The authors declare that they have no known competing financial interests or personal relationships that could have appeared to influence the work reported in this paper.

Appendix. NLP sensitivity update

In this section, we show how to solve the parametric sensitivity updated for $V_p(\hat{\mathbf{x}}_{t+1|t})$. We note that the OCP (20) is parametric in the initial condition $p := \hat{\mathbf{x}}_t$, which is rewritten as a generic parametric NLP:

$$\mathcal{P}(p): \quad \min_w J(w,p), \quad \text{s.t. } c(w,p) = 0, \quad g(w,p) \le 0 \tag{A.1}$$

where w denotes the primal variables, p denotes the parameter, J denotes the cost, c denotes the equality constraints and g denotes the inequality constraints. The NLP (A.1) is solved with $p = p_0$. We denote the Lagrangian of (A.1) as,

$$\mathcal{L}(w, p_0, \lambda, \nu) := J(w, p_0) + \lambda^T c(w, p_0) + \nu^T g(w, p_0) \tag{A.2}$$

Let the primal–dual solution vector be represented as $\mathbf{s}^* := [w^{*^T}, \lambda^{*^T}, \nu^{*^T}]^T$ and assume that it satisfies linear independent constraint qualification (LICQ), strong second order sufficient conditions (SSOSC), and strict complementarity i.e., $\nu_i - g_i(w^*) > 0$ for all i. We define $g_{\mathbb{A}}(w)$ as the sub-vector of g with all $g_i(w^*) = 0$. If the functions J, c, and g are sufficiently differentiable w.r.t w and p in a neighborhood of the nominal solution $\mathbf{s}^*(p_0)$, for $\mathcal{P}(p_0)$, then for p in the neighborhood of p_0, $\exists\, \mathbf{s}^*(p)$ which is continuous and differentiable and a unique local minimizer of the problem $\mathcal{P}(p)$. In this case, the sensitivity can be computed by applying the implicit function theorem (IFT) on the KKT conditions of (A.1) as detailed in [26], which results in

$$\left(\mathcal{M}\frac{\partial \mathbf{s}^*}{\partial p} + \mathcal{N}\right)(p - p_0) \approx 0 \tag{A.3}$$

where

$$\mathcal{M} := \begin{bmatrix} \nabla_{ww}\mathcal{L}(\mathbf{s}^*(p_0)) & \nabla_w c(w^*(p_0)) & \nabla_w g_{\mathbb{A}}(w^*(p_0)) \\ \nabla_w c(w^*(p_0))^T & 0 & 0 \\ \nabla_w g_{\mathbb{A}}(w^*(p_0))^T & 0 & 0 \end{bmatrix}$$

is the KKT matrix and

$$\mathcal{N} := \begin{bmatrix} \nabla_{wp}\mathcal{L}(\mathbf{s}^*(p_0)) \\ \nabla_p c(w^*(p_0))^T \\ \nabla_p g_{\mathbb{A}}(w^*(p_0))^T \end{bmatrix}$$

Changes in active constraint sets can be handled by solving a predictor–corrector QP using a path following strategy as explained in [20]. In this case, Algorithm 2 would solve a predictor–corrector QP, instead of (A.3) to compute $\mathbf{s}^*(\hat{\boldsymbol{x}}_{t+1|t})$.

References

[1] D.E. Seborg, D.A. Mellichamp, T.F. Edgar, F.J. Doyle III, Process Dynamics and Control, John Wiley & Sons, 2010.
[2] J.B. Rawlings, R. Amrit, Optimizing process economic performance using model predictive control, in: Nonlinear Model Predictive Control, Springer, 2009, pp. 119–138.
[3] D.R. Bartusiak, NLMPC: A platform for optimal control of feed-or product-flexible manufacturing, in: Assessment and Future Directions of Nonlinear Model Predictive Control, Springer, 2007, pp. 367–381.
[4] L.T. Biegler, Efficient solution of dynamic optimization and NMPC problems, in: Nonlinear Model Predictive Control, Springer, 2000, pp. 219–243.
[5] M. Campos, H. Teixeira, F. Liporace, M. Gomes, Challenges and problems with advanced control and optimization technologies, IFAC Proc. Vol. 42 (11) (2009) 1–8.
[6] L.O. Santos, P.A. Afonso, J.A. Castro, N.M. Oliveira, L.T. Biegler, On-line implementation of nonlinear MPC: an experimental case study, Control Eng. Pract. 9 (8) (2001) 847–857.
[7] R. Findeisen, F. Allgöwer, Computational delay in nonlinear model predictive control, IFAC Proc. Vol. 37 (1) (2004) 427–432.
[8] W.-H. Chen, D.J. Ballance, J. O'Reilly, Model predictive control of nonlinear systems: Computational burden and stability, IEEE Proc. D 147 (4) (2000) 387–394.
[9] D.W. Griffith, L.T. Biegler, S.C. Patwardhan, Robustly stable adaptive horizon nonlinear model predictive control, J. Process Control 70 (2018) 109–122.
[10] M. Ellis, H. Durand, P.D. Christofides, A tutorial review of economic model predictive control methods, J. Process Control 24 (8) (2014) 1156–1178.
[11] R. Shekhar, Variable Horizon Model Predictive Control: Robustness and Optimality (Ph.D. thesis), University of Cambridge, 2012.
[12] L. Grüne, J. Pannek, Nonlinear model predictive control, in: Nonlinear Model Predictive Control, Springer, 2017, pp. 45–69.
[13] D. Angeli, R. Amrit, J.B. Rawlings, On average performance and stability of economic model predictive control, IEEE Trans. Autom. Control 57 (7) (2011) 1615–1626.
[14] D. Angeli, J.B. Rawlings, Receding horizon cost optimization and control for nonlinear plants, IFAC Proc. Vol. 43 (14) (2010) 1217–1223.
[15] M. Diehl, R. Amrit, J.B. Rawlings, A Lyapunov function for economic optimizing model predictive control, IEEE Trans. Automat. Control 56 (3) (2011) 703–707.
[16] L. Grüne, Economic receding horizon control without terminal constraints, Automatica 49 (3) (2013) 725–734.
[17] T. Faulwasser, M. Korda, C.N. Jones, D. Bonvin, On turnpike and dissipativity properties of continuous-time optimal control problems, Automatica 81 (2017) 297–304.
[18] R. Huang, E. Harinath, L.T. Biegler, Lyapunov stability of economically oriented NMPC for cyclic processes, J. Process Control 21 (4) (2011) 501–509.
[19] R. Amrit, J.B. Rawlings, D. Angeli, Economic optimization using model predictive control with a terminal cost, Annu. Rev. Control 35 (2) (2011) 178–186.
[20] J. Jäschke, X. Yang, L.T. Biegler, Fast economic model predictive control based on NLP-sensitivities, J. Process Control 24 (8) (2014) 1260–1272.
[21] D.W. Griffith, V.M. Zavala, L.T. Biegler, Robustly stable economic NMPC for non-dissipative stage costs, J. Process Control 57 (2017) 116–126.
[22] C.G. Economou, M. Morari, B.O. Palsson, Internal model control: Extension to nonlinear system, Ind. Eng. Chem. Process Des. Dev. 25 (2) (1986) 403–411.
[23] J.A.E. Andersson, J. Gillis, G. Horn, J.B. Rawlings, M. Diehl, CasADi – A software framework for nonlinear optimization and optimal control, Math. Program. Comput. (In Press, 2018).
[24] A. Wächter, L.T. Biegler, On the implementation of an interior-point filter line-search algorithm for large-scale nonlinear programming, Math. Program. 106 (1) (2006) 25–57.
[25] T.J. Williams, R.E. Otto, A generalized chemical processing model for the investigation of computer control, Trans. Am. Inst. Electr. Eng. I: Commun. Electron. 79 (5) (1960) 458–473.
[26] A.V. Fiacco, Sensitivity analysis for nonlinear programming using penalty methods, Math. Program. 10 (1) (1976) 287–311.